Design of potent and selective GSK3β inhibitors with acceptable safety profile and pharmacokinetics

Dominique Lesuisse [a,*], Gilles Tiraboschi [c], Alain Krick [d], Pierre-Yves Abecassis [d], Gilles Dutruc-Rosset [a], Didier Babin [a], Frank Halley [a], Fabienne Châtreau [a], Sylvette Lachaud [a], Alain Chevalier [a], Dominique Quarteronet [b], Marie-Claude Burgevin [b], Céline Amara [d], Philippe Bertrand [b], Thomas Rooney [b]

[a] Medicinal Chemistry, Sanofi-aventis, 13 Quai Jules Guesde, 94300 Vitry-sur-Seine, France
[b] CNS Department, Sanofi-aventis, 13 Quai Jules Guesde, 94300 Vitry-sur-Seine, France
[c] Molecular Modelling, Sanofi-aventis, 13 Quai Jules Guesde, 94300 Vitry-sur-Seine, France
[d] DMPKS, Sanofi-aventis, 13 Quai Jules Guesde, 94300 Vitry-sur-Seine, France

ARTICLE INFO

ABSTRACT

From potent and selective inhibitors of GSK3β displaying CYP1A2 inhibition and poor PK properties, mostly linked to metabolic instability and in vivo hydrolysis of the amide bond, we were able to obtain safe and orally available inhibitors with good half lives.

© 2010 Elsevier Ltd. All rights reserved.

Glycogen synthase kinase beta (GSK3β)[1] is involved in phosphorylation of at least two physiologically important proteins, tau[2] and glycogen synthase.[3] These proteins have been shown to be intimately associated with some pathological processes, such as Alzheimer's disease[4] and diabetes, respectively. In the course of a programme aimed at finding inhibitors of this enzyme, we conducted a high throughput and identified a hit **1** with inhibitory activity in the micromolar range. The optimisation of the potency and the selectivity of this hit led to the identification of two potent aminoindazoles **4** and **5**.[5] However, as is often the case in medicinal chemistry, optimization of the potency was paralleled by a decrease of the physicochemical properties of the compounds. Table 1 illustrates how some of these properties, such as solubility, lipophilicity and protein binding got worse through each step of potency optimization from 1 to 4 and 5. We therefore anticipated that there could be potential ADME issues to solve with these first leads. The object of the present paper is to describe how we transformed these potent leads into safe and orally available compounds with acceptable PK properties, including brain exposure.

One of the important hurdles in medicinal chemistry is to identify compounds with a good safety profile. Inhibition of hepatic cytochrome P450 enzymes and the hERG potassium channel are among the most serious safety issues, since this can result in drug–drug interactions[7] and cardiac toxicity (QT prolongation[8]), respectively. We also analyzed our compounds in assays predictive of genotoxicity or clastogenicity. In order to gain insight into the optimization for these series, we profiled **4** and **5** in a series of early ADME and toxicity assays. The results are displayed in Table 2.

Although the stability in human S9 hepatic fractions was good, the metabolic stability in mice S9 hepatic fractions was poor and so the optimization of this parameter, predictive of high clearance in rodents, was undertaken. No problem was anticipated regarding hERG channel inhibition, Ames, CYP 3A4, 2D6, 2C9 and 2C19 inhibition. However, the compounds displayed potent CYP1A2 inhibition. The chemical optimization programme was therefore also focused on lowering this CYP1A2 inhibition.

After evaluation of ∼60 GSK3β inhibitors on a panel of hepatic CYP isoforms (human recombinant), about two thirds displayed inhibition of Cyp1A2, whereas inhibition of the other Cyp isoforms did not appear to represent a major issue (Table 3). Inhibition of Cyp1A2 was therefore identified as a persistent series-related issue that would need to be addressed early on.

In addition to the screening CYP panel used above, we evaluated some of the most potent GSK3β inhibitors on a kinetic CYP1A2 assay to confirm their inhibition[9] and check for potential

* Corresponding author. Tel.: +33 1 58 93 37 71; fax: +33 1 58 93 34 50.
E-mail address: dominique.lesuisse@sanofi-aventis.com (D. Lesuisse).

Table 1
Evolution of the physicochemical properties of the compounds along the optimization process

Compd	**1**	**2**	**3**	**4**	**5**
GSK3β (μM)[6]	0.94	0.44	0.040	0.005	0.006
Sol (mg/ml)	0.716	0.168	0.067	<0.001	<0.001
Log D pH 7.4	<1	2.2	3.05	3.86	4.39
% HSA binding	<90	92.8	97.3	99.3	99.4

Table 2
Full early ADME-T profile of **4** and **5**

Compd	Sol (mg/ml)	Met stab[a,b]	Met stab[a,c]	Caco$_2$ % Transp/h	CYP1A$_2$[d] IC$_{50}$ (μM)	CYP3A$_4$[d] IC$_{50}$ (μM)	CYP2D$_6$[d] IC$_{50}$ (μM)	CYP2C$_9$[d] IC$_{50}$ (μM)	CYP2C$_{19}$[d] IC$_{50}$ (μM)	Ames	hErg % inh 10 μM
4	<0.019	10	91	NR[d]	0.07	>10	>10	>10	>10	NR[e]	7
5	<0.016	40	91	3.9	0.08	>10	>10	>10	>10	Negative	24

[a] Percent of compound remaining after 15 min of S9 fraction exposure.
[b] Mouse S9 hepatic fraction.
[c] Human S9 hepatic fraction.
[d] Human recombinant CYP enzymes.
[e] No result.

Table 3
Statistics of CYP isoforms inhibition by the first inhibitors of the programme

CYP isoform	Number of compounds		
	IC$_{50}$ > 10 μM	IC$_{50}$ < 10 μM	IC$_{50}$ < 1 μM
3A4	60	6	0
1A2	26	29	22
2C9	31	7	0
2D6	57	6	0
2C19	57	7	0

time-dependency.[10] The trend for CYP1A2 inhibition was particularly pronounced in our most interesting series of GSK3β inhibitors,[11] as can be seen from Table 4. In addition, some of our potent GSK3β inhibitors displayed time-dependent kinetics of CYP1A2 inhibition, suggesting a mechanism-based inhibition leading to covalent binding to the enzyme. One of these compounds (**8**) incorporated a furan ring in the molecule. This motif has been reported to lead to covalent binding to CYP enzymes via formation of reactive intermediates, such as epoxides and oxirenes, or the production of open 1,4-diketone derivatives.[12] The phenol

Table 4
CYP1A2 inhibition of 5- and 6-substituted aminoindazoles[8,9]
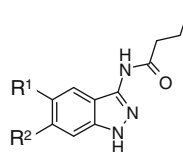
R^1	R^2	Compd	GSK3β (μM)	CYP1A$_2$[a] (μM)	CYP1A$_2$[b] (μM)	Slope[c]
Br	4-HOPh	**4**	0.005	>10	0.07	−1
Ph	Cl	**5**	0.006	<0.4	0.08	−1
4-H$_2$NPh	Cl	**6**	0.007	0.98		
4-HOPh	Cl	**7**	0.008		0.08	−2
3-Furyl	Cl	**8**	0.011	<0.4	0.03	−3
4-MePh	Cl	**9**	0.012	1.75		
4-FPh	Cl	**10**	0.016	0.83	0.13	1
4-NO$_2$Ph	Cl	**11**	0.017	4.46		
4-BnOPh	Cl	**12**	0.022	>10		
Br	Cl	**13**	0.055	0.55		
H	4-HOPh	**3**	0.036	>50	22	−2
H	3-Thienyl	**14**	0.93	1.9		
H	Ph	**15**	1.28	>10	0.39	0
H	3,5-F2-Ph	**16**	2.9	13.8	2.7	−3
H	3-Py	**17**	11	1.2	5.9	0

[a] CYP1A$_2$ screening panel.
[b] CYP1A$_2$ kinetic assay.[8]
[c] % IC$_{50}$/min.

analogues **3** and **7** also displayed some time-dependency, but to a lesser extent (slope −2%/min).

CYP1A2 is involved in the metabolization of planar highly conjugated compounds.[13] A homology model built from bacterial CYP1A2 has been reported showing that the heme pocket of the enzyme is small and lined with aromatic amino acids.[14] A π–π stacking between aromatics and the enzyme[15] has been suggested to explain why most substrates or inhibitors of this enzyme are relatively small-sized, flat and aromatic compounds. This preference for small compounds could explain the loss of CYP1A2 inhibition with bulkier **12**. However, it was difficult to rationalize the difference in CYP1A2 inhibition properties between **5** and **9**, or between **6** and **11** according to the above rules. The molecular reasons for competitive 1A2 inhibition did not appear to be solely linked to the propyl amide side chain or to the GSK3β inhibiting activity, as compounds **3** and **12**, displaying the same chain and potency, were totally devoid of 1A2 inhibition.

Although it is less well described for CYP1A2 than for CYP3A4, lipophilicity is also linked to recognition by the CYP enzymes. Several reports in the literature point to a relationship between log *P* and CYP inhibition.[16] This could also be seen in our own series when comparing compounds **1** with **13** (Table 5).
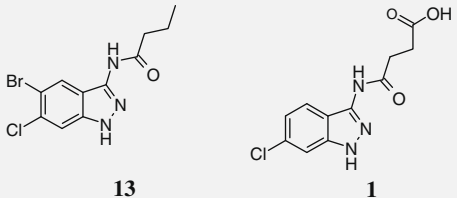
As this inhibition is multiparametric, we went on to build a QSAR model to better predict potential inhibitors. A few QSAR models of CYP1A2 have been described in the literature;[17] however it is often better to rebuild a model suited to the particular series involved. A set of 29 compounds ranging from active (IC$_{50}$ 32 nM) to inactive (IC$_{50}$ 73 μM) in the CYP1A2 kinetic assay were used to build a QSAR CoMFA model.[18] For each compound, the best minimized conformations were aligned superimposing their common substructures, as depicted in Figure 1. The final selected model displayed an optimal number of four components using only the steric fields as CoMFA descriptors. The correlation graph of the predicted activities is shown in Figure 2.
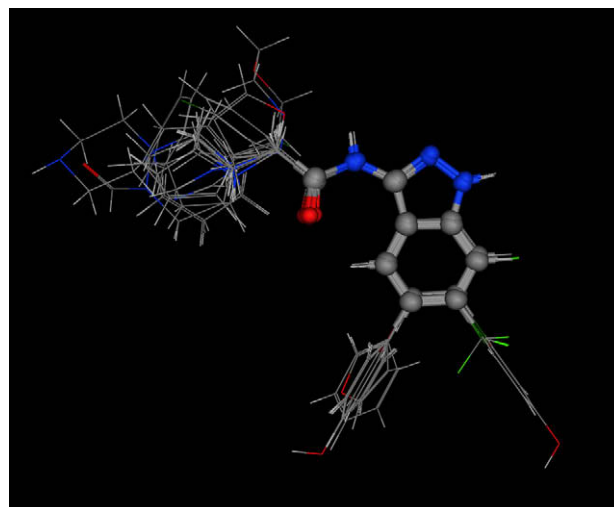
More practically for the medicinal chemist, the model provided a chemical interpretation (Fig. 3). In the CoMFA model the contour maps sterically unfavourable and favourable regions are shown in green and yellow, respectively, clearly predicting that bulky groups on the 3-side chain should prevent CYP 1A2 inhibition. From our model, bulky positions 5- and 6- of the aminoindazole could enhance CYP1A2 inhibition. However, as depicted in Figure 1, no large chemical diversity was explored in these positions in our dataset. Interpretation of our model for these regions has therefore to be taken cautiously.

This model was used throughout the programme to predict the compounds to be prepared and led to the design of potent inhibitors devoid of CYP1A2 inhibition.

The second aim of our optimization was focused on obtaining good exposure of the inhibitors. Brain exposures were also monitored as we were looking for brain penetrant compounds for Alzheimer's disease and related neurodegenerative disorders.

Figure 1. The aligned compounds used to generate the CoMFA model of CYP1A2 inhibition. The common substructure (depicted in ball and stick) was used for the alignment.
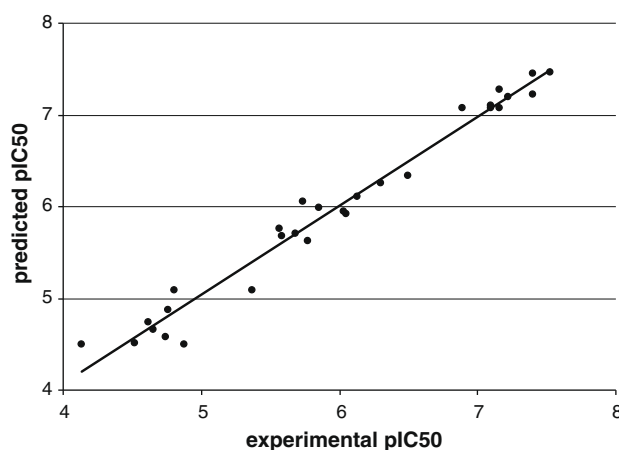
Figure 2. Correlation between experimental and CoMFA predicted activities. The kinetic CYP1A2 inhibition data are expressed in pIC$_{50}$ were pIC$_{50}$ = −Log (IC$_{50}$).

Bulky groups Prevent inhibition
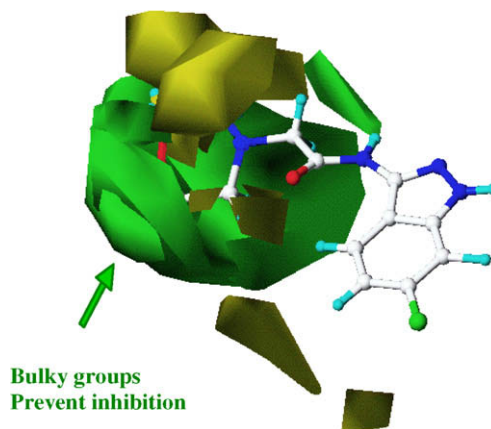
Figure 3. Chemical interpretation of the COMFA model. Contour maps for the sterical field depicted around aminoindazole scaffold highlight the influence of the bulk on aminoindazole on the CYP1A2 inhibition properties. Compounds **20** is depicted with an experimental pIC$_{50}$ = 4.80688 and predicted pIC$_{50}$ = 5.08664. Unfavourable regions are in green and favourable regions are in yellow.

Table 5
CYP1A$_2$ inhibition as a function of lipophilicity

	13	**1**
GSK3β	0.055 μM	0.94 μM
Log D pH 7.4	3.66	<1
CYP1A2	0.55 μM	>50 μM

Compounds **4** and **5** along with several related analogs were evaluated in vivo in mouse preliminary pharmacokinetic studies to assess the general pharmacokinetic parameters of this series. To increase the throughput we used cassette dosing so the data have to be viewed as preliminary pharmacokinetic results. The results of some of these studies (Table 6) showed that at least some of the compounds (e.g., **5**, **8**, **13** and **18**) displayed good or acceptable brain/plasma ratios, indicating that this parameter was not limiting for these series. However, the data also pointed to very low exposure and low, or non-measurable, bioavailability for all compounds. As the permeability of the compounds was generally good, as shown by their results in the Caco2 assay, these liabilities were hypothesized to be mainly linked to their poor metabolic stability in mice, as reflected by their high clearances. However, this parameter was not the only driver of poor exposure, as shown by compound **13** which, despite good permeability and metabolic stability in mice, displayed extremely high clearance and low plasma exposure. Even compound **19** with acceptable clearance, in agreement with its in vitro metabolic stability, displayed a short half-life.

The emphasis of the optimization program was therefore focused on understanding and improving the parameters controlling the rodent half-life and exposure, especially the metabolic stabilities of these compounds.

The compounds that had been optimized for potency and selectivity were very lipophilic and poorly soluble. Even though the correlation is not absolute, these properties have been shown to be generally associated with high uptake by liver metabolizing enzymes (CYP's), resulting in higher metabolism and clearance.[19] Modulation of these properties via the 3-position chain was in theory possible, as it had been shown to be exposed to the solvent area of the kinase and therefore large modifications should be possible without changing the potency.[5] An acidic moiety is ideal to solubilise and protect from metabolism,[20] but the ability of an acidic compound to penetrate the brain by passive diffusion is limited, as was confirmed on **1** (Table 7) which displayed brain levels at the limit of detection. Earlier data on **20** incorporating a basic side chain, showed better brain exposure but the short half-life was not predicted by the

metabolic stability and was not acceptable for in vivo dosing. Two analogues of **5**, **21** and **22**, incorporating such basic side chains were also investigated and displayed very short half-lives despite high metabolic stability (Table 7).

The absence of correlation between S9 mice metabolism and in vivo clearance posed a problem. At least two types of chemical modification could account for this discrepancy. The first is a direct glucuroconjugation of the compound on any of its nucleophilic positions. In the case of our series it could be the N1 or N3 positions of the aminoindazole. There are precedents in the literature supporting direct N-glucuroconjugation on several heterocycles, such as imidazoles and triazoles.[21] One way to quantitate the extent of oxidative (phase I) versus glucuroconjugation (phase II) metabolism is to compare their transformation in mouse liver microsomes in the presence and absence of NADPH and UDPGA, the co-factors necessary for the oxidative and conjugative metabolism, respectively. This experiment was performed on a few selected compounds (data not shown) and the results suggested that, at least for these compounds, direct glucuroconjugation was not involved in the metabolization.

The second type of chemical modification that could be responsible for the poor half-life is hydrolysis of the amide bond. Throughout the program, the clearance data obtained with amides were in relatively good agreement with the expected ease of amide chemical hydrolysis, that is, primary > secondary > aromatic. In vivo this hydrolysis could be achieved by several processes: phase I metabolism (CYP enzymes,[22] hydrolases, peptidases) or even chemically. The compounds were shown to be stable to chemical hydrolyses and in mouse plasma (data not shown). To avoid a possible issue of amide hydrolysis, we explored replacement of this function by non-hydrolysable substitutions. Some examples are displayed in Table 8. Complete removal of the amide group, as in **23**, or replacement by alkyl or aryl groups, such as compounds **24–28**, proved detrimental to activity, as predicted by molecular modelling, since the carbonyl function had been shown to make a hydrogen bond accepting interaction with the hinge binding portion of the kinase.[5] More stable replacements able to keep this interaction, such as carbamates **29–32** and ureas **33–35**, displayed better inhibitory activity.

Table 6
Full ADME and pharmacokinetic (PK)[a] profile of 5-, 6- and 7-substituted aminoindazoles
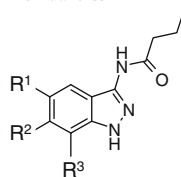
R^1	R^2	R^3	Compd	GSK3β (μM)	Sol[b] (μg/ml)	Log D pH 7.4	Met stab[c] H[d]	M[e]	Caco$_2$ (T/h)	Cp$_{max}$[f] (ng/ml)	Cb$_{max}$[f] (ng/g)	Cl[g] (l/h/kg)	T$_{1/2}$[g] (h)	B/P[h]	F (%)
Br	4-HOPh		4	0.005	<20	4.4	91	10	NR	12		3.3	0.3		1
Ph	Cl		5	0.006	<20	3.7	91	40	3.9	11	8	6.9	0.2	1.2	
4-HOPh	Cl		7	0.008	<20	3.9	NR	19	8.02	5		8	1.3		
3-Furyl	Cl		8	0.011	<20	4.1	45	4	12.3	6		15.5	0.3	0.5	
Br	Cl		13	0.024	<20	4.4	97	87	17.25	1		9	0.1	2	
	4-HOPh		3	0.055	67	3.7	58	4	15.25	14		2.7	0.4	0.1	
Ph	F	F	18	0.005	4	2.4	86	56	nd	34	50	4.5	0.3	1.7	
	F	F	19	0.270	54	3.0	98	93	16.33	172	56	1.2	0.3	0.3	18

[a] Mice 1 mg/kg oral and iv cassette dosing.
[b] Nephelometry.
[c] Percent of compound remaining after 15 min of S9 fraction exposure.
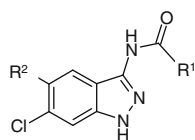[d] Human.
[e] Mice.
[f] Oral dosing.
[g] Plasma, iv dosing.
[h] iv dosing.

Table 7
ADME and pharmacokinetic (PK)[a] profile of aminoindazoles with various acidic or basic chains in 3-position (R^1)

R^1	R^2	Compd	GSK3β (μM)	Sol[b] (μg/ml)	Log D pH 7.4	Met stab[c]		Caco$_2$ (T/h)	Cp$_{max}$[f] (ng/ml)	Cb$_{max}$[g] (ng/g)	Cl (l/h/kg)	$T_{1/2}$[f] (h)	B/P[g]	F (%)
						M[d]	H[e]							
CH$_2$CH$_2$COOH		**1**	0.94	>134	<1.2	94	100	0.39	179	7[h]	1	2.2	nc	48
CH$_2$N–Morpholyl		**20**	0.99	<20	3.1	nd	nd		283	246	1.3	0.4	0.3[f]	36
CH(Me)N–Piperidinyl	Ph	**21**	0.025	<20	3.53	100	85	nq	40	832	9.7	0.8	6.2	nc
CH$_2$N–Morpholyl	Ph	**22**	0.051	28	3.49	100	91	5.56	44	1278	5.9	0.5	2.6	28

[a] Mice 1 mg/kg oral and iv cassette dosing.
[b] Nephelometric solubility.
[c] Percent of compound remaining after 15 min of S9 fraction exposure.
[d] Mice.
[e] Human.
[f] Oral dosing.
[g] iv dosing.
[h] 0.5 mpk iv.

Table 8
GSK3β inhibition of aminoindazole incorporating non-amide chains in 3-position
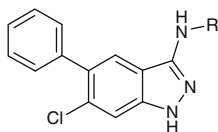
R	Compd	GSK3β (μM)
H	**23**	0.47
Butyl	**24**	0.8
2-Pyridyl	**25**	0.21
4-CF3Ph	**26**	2.00
6-Meo-2-pyridyl	**27**	0.1
5-NO$_2$-2-pyridyl	**28**	0.74
COOiBu	**29**	0.12
COOAllyl	**30**	0.1
COOBn	**31**	0.13
COOMe	**32**	0.21
CONH$_2$	**33**	0.125
CONHBn	**34**	0.055
CONHiPr	**35**	0.05

Several ureas presented the desired potency on GSK3β and metabolic stability and a set of the most active ones **36–39** were selected for PK studies (Table 9).

Some of these compounds displayed some good PK features with low clearance and good bioavailability (**38** and **39**). Only **39** displayed acceptable brain exposure. It was evaluated against a panel of 28 kinases, including Cdk2, Cdk4 and Cdk5 and was found inactive (<50% at 10 μM), except for Cdk9 (81% at 10 μM[23]). It displayed a level of CYP1A2 inhibition that was considered as acceptable (2.2 μM) and no hERG channel inhibition (IC$_{50}$ > 10 μM). This compound was kept for further evaluation.

We also examined the ability of the compounds to inhibit tau phosphorylation on serine-396 in cortex slices.[24] There was generally a good correlation between GSK3β inhibition and inhibition of tau phosphorylation with compounds <20 nM for inhibition of GSK3β displaying inhibition of tau phosphorylation at <μM level. This value was set as a threshold for further compound selection. Compound **39** displayed good potency in this assay with an IC$_{50}$ of 270 nM. It was therefore engaged in vivo studies where it was shown to inhibit the phosphorylation of tau at the selective

Table 9
GSK3β inhibition, solubility, metabolism and pharmacokinetic (PK)[b] data of best ureas derived from **5**
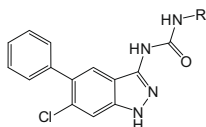
R				
	36	**37**	**38**	**39**
Compd	GSK3β nM	Sol[a] (μg/ml)	S9 Mice	Cl	$T_{1/2}$	AUCp (h ng/g)	B/P	F (%)
---	---	---	---	---	---	---	---	---
36	12	<20	85	2.2[c]	0.2[c]	449[c]	0.04[c]	–
37	25	>208	100	5.5	1.3	180	nc	nc
38	29	<20	79	0.1	1.2	8738	0.01	78
39	65	<20	92	1.1	1.7	906	0.2	37

[a] Nephelometric solubility.
[b] Mice, cassette dosing, 1mpk iv.
[c] Single PK iv 1mpk of the chlorohydrate salt.

GSK-3β epitope (pSer396/404) by 21–53% for up to 2 h when administered by oral route at 10 mg/kg.

The CYP1A2 inhibition and metabolic clearance of a series of 3-aminoindazoles was optimized by chemical variations at the 3-position. It was shown that the hydrolysis of the amide bond partly accounts for the high clearance of some of these compounds.

Acknowledgements

We are grateful to the analytical department for compound analyses.

Supplementary data

Supplementary data associated with this article can be found, in the online version, at doi:10.1016/j.bmcl.2010.01.132.

References and notes

1. Frame, S.; Cohen, P. *Biochem. J.* **2001**, *359*, 1. and references cited therein.
2. Flaherty, D. B.; Soria, J. P.; Tomasiewicz, H. G.; Wood, J. G. *J. Neurosci. Res.* **2000**, *62*, 463.
3. Ferrer, J. C.; Favre, C.; Gomis, R. R.; Fernandez-Novell, J. M.; Garcia-Rocha, M.; De La Iglesia, N.; Cid, E.; Guinovart, J. J. *FEBS Lett.* **2003**, *546*, 127.
4. Maccioni, R. B.; Munoz, J. P.; Barbeito, L. *Arch. Med. Res.* **2001**, *32*, 367.
5. Lesuisse, D.; Dutruc-Rosset, G.; Tiraboschi, G.; Dreyer, M. K.; Maignan, S.; Chevalier, A.; Halley, F.; Bertrand, P.; Burgevin, M.-C.; Quarteronet, D.; Rooney, T. *Bioorg. Med. Chem. Lett.* **2010**, *20*, 1985.
6. *Technical note*: measurement of GSK3β enzymatic activity by Scintillation Proximity Assay (SPA). Partially purified recombinant human GSK3β enzyme is incubated for 30 min at 20 °C in 96-W microplates with 1 μM ATP (including 50 nCi γ-[^{33}P]-33P]-ATP/well) and 0.8 μM of pGS-2 peptide substrate (Upstate Biotechnology Inc.) in the presence of tested compound, and in HEPES buffer (40 mM, pH 7.4, supplemented with 200 μM EDTA, 10 mM MgCl$_2$, 1 mM DTT and 0.1 ml/ml BSA). Enzymatic reaction is stopped by adding SPA-streptavidine beads (GE Healthcare) concentrated (6 mg/ml) in PBS (containing 20 mM ATP, 25 mM EDTA and 0.2% triton X-100) under 10 min. agitation. Radioactivity is measured by using a scintillation liquid reader (1450 Microbeta™, Perkin–Elmer). IC$_{50}$ values are calculated by non-linear regression analysis with Excel/XL fit software (IDBS).
7. Murray, M. *Int. J. Mol. Med.* **1999**, *3*, 227.
8. Jalaie, M.; Holsworth, D. D. *Mini-Rev. Med. Chem.* **2005**, *5*, 1083.
9. Data from screening panel have to be taken cautiously as false negative results could be obtained with insoluble compounds. This can be seen for instance with compounds **4** and **15**.
10. Two protocols were used to determine CYP1A2 inhibition (Supplementary data 2). Briefly: *Panel rhCYP1A2 assay*: evaluation of the inhibitory potency of new chemical entities using human recombinant CYP's. Probe substrate by determination of IC$_{50}$'s, in order, to investigate potential drug–drug interactions. CYP1A2 probe substrate 3-cyano-7-ethoxycoumarine (CEC) concentration: 0.4–50 μM. Fluorescent: Ex-410 nm Em-460 nm. *Kinetic rhCYP1A2 assay*: evaluation of the reversible and irreversible inhibitory potency of new chemical entities using human recombinant CYP's. Probe substrate kinetics IC$_{50}$ determination from 0 to 15 min in order to investigate potential drug–drug interactions. Potential for irreversible inhibition being determined as IC$_{50}$ time course variation; CYP1A2 probe substrate 3-cyano-7-ethoxycoumarine (CEC) concentration: 0.002–40 μM. Fluorescent: Ex-410 nm Em-460 nm.
11. The synthesis of the compounds is described in: Dutruc-Rosset, G.; Lesuisse, D.; Rooney, T.; Halley, F. FR 2836915 A1; PCT Patent Publication No. WO2003/078403 A2; *Chem. Abstr.* **2003**, *139*, 246027.; Lesuisse, D.; Dutruc-Rosset, G.; Halley, F.; Babin, D.; Rooney, T.; Tiraboschi, G. PCT Patent Publication No. WO2004/062662 A1; *Chem. Abstr.* **2004**, *141*, 140438.; Lesuisse, D.; Dutruc-Rosset, G.; Halley, F.; Babin, D.; Rooney, T. PCT Patent Publication No. WO2004/022544 A; *Chem. Abstr.* **2004**, *140*, 253562.
12. Fontana, E.; Dansette, P. M.; Poli, S. M. *Curr. Drug Metab.* **2005**, *6*, 413; Zhou, S.; Chan, S. Y.; Goh, B. C.; Chan, E. i.; Duan, W.; Huang, M.; McLeod, H. L. *Clin. Pharmacokinet.* **2005**, *44*, 279.
13. Lopez-de-Brinas, E.; Lozano, J. J.; Centeno, N. B.; Segura, J.; Gonzalez, M.; de la Torre, R.; Sanz, F. Molecular Modeling and Prediction of Bioactivity, In *Proceedings of the European Symposium on Quantitative Structure–Activity Relationships: Molecular Modeling and Prediction of Bioactivity*, 12th ed.; Copenhagen, Denmark, Aug. 23–28, 1998 (**2000**), Meeting Date 1998, 141–146. Kluwer Academic/Plenum: New York, NY.
14. Lewis, D. F.; Lake, B. G.; George, S. G.; Dickins, M.; Eddershaw, P. J.; Tarbit, M. H.; Beresford, A. P.; Goldfarb, P. S.; Guengerich, F. P. *Toxicology* **1999**, *139*, 53.
15. Lewis, D. F. V.; Modi, S.; Dickins, M. *Drug Metab. Rev.* **2002**, *34*, 69.
16. Riley, R. J.; Parker, A. J.; Trigg, S.; Manners, C. N. *Pharm. Res.* **2001**, *18*, 652.
17. See for instance: Korhonen, L. E.; Rahnasto, M.; Maehoenen, N. J.; Wittekindt, C.; Poso, A.; Juvonen, R. O.; Raunio, H. *J. Med. Chem.* **2005**, *48*, 3808; Lewis, D. F. V.; Lake, B. G.; Dickins, M. *Xenobiotica* **2004**, *34*, 501.
18. The compounds are ionized simulating a water solution at pH 7.5 using the pK$_a$ predicted with ACD/pK$_a$ DB (ACD/pK$_a$ DB version 8.0. Advanced Chemistry Development Inc., Toronto ON, Canada, www.acdlabs.com, 2004). A conformational search was performed using the MMF94s forcefield as implemented in Molecular Operating Environment (MOE) software. (MOE, 2004.03; Chemical Computing Group Inc.: Montreal, Quebec Canada, 2004). The 3D QSAR models were generated by the standard CoMFA method implemented in SYBYL 7.0 (SYBYL®, version 7.0, 1699, Tripos Inc., South Hanley, St. Louis, Missouri 63144). A series of regression analysis were performed using the partial least square method and cross validated using the leave-one-out method using steric or electrostatic or both calculated fields as descriptors. IC$_{50}$'s obtained in the kinetic CYP1A2 assay were converted in pIC$_{50}$ (where pIC$_{50}$ = −Log (IC$_{50}$)) and taken as dependent variables to generate the models. The final selected model displayed an optimal number of four components (r^2 = 0.97; q^2 = 0.87; SD = 0.2) using only the steric fields as CoMFA descriptors). The list the of compounds and their predicted pIC$_{50}$ are reported in Supplementary data Table 1. Due to the limited number of available data no external validation set could be designed.
19. van de Waterbeemd, H.; Smith, D. A.; Beaumont, K.; Walker, Don K. *J. Med. Chem.* **2001**, *44*, 1313.
20. Gleeson, M. P. *J. Med. Chem.* **2008**, *51*, 817.
21. Huskey, S.-E. W.; Doss, G. A.; Miller, R. R.; Schoen, W. R.; Chiu, S.-Hing. *Drug Metab. Disposit.* **1994**, *22*, 651.
22. Lewis, D. F. V. *Guide to Cytochrome P450. Structure and Function*, Taylor & Francis (August 2001) p 77.
23. This particular assay is performed at very low ATP concentration (1 μM) and any IC$_{50}$ above 50 nM is considered safe versus transcription inhibition.
24. Briefly, brain slices (300 μm) are prepared from cerebral cortex of 10 week-old rats, and slice suspension (50 μl/microtube) is incubated in DMEM (containing pyruvate and 4.5 g/l glucose) with tested compound in a final volume of 500 μl, for 120 min at 37 °C under mild agitation. Incubation is stopped by centrifugation, followed by lysis and sonication at 4 °C. Lysates are then centrifuged (18,000g, 15 min, 4 °C), and the supernatants are used for protein dosage, and subsequent western blotting analysis. SDS–PAGE electrophoresis is performed in MOPS–SDS denaturating conditions; the phosphorylation of tau protein is detected by using AD2 mouse monoclonal antibody specific for Ser396/404 phosphoepitope as primary antibody, and peroxydase-labelled mouse antiserum as secondary antibody for measuring signal by chemioluminescence. Analysis of autoradiogrammes by 'GeneTools' software (Syngene, GeneGnome, Ozyme) was performed for IC$_{50}$ estimation.